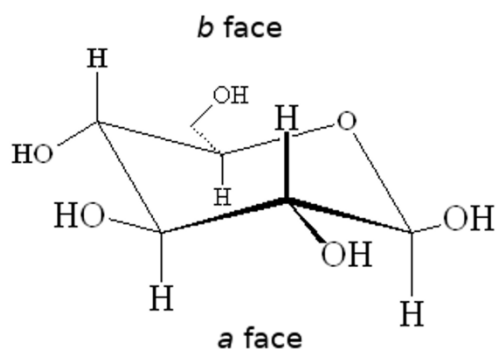


Supplementary material for the article:

Stanković, I. M.; Blagojević Filipović, J. P.; Zarić, S. D. Carbohydrate – Protein Aromatic Ring Interactions beyond CH/ $\pi$  Interactions: A Protein Data Bank Survey and Quantum Chemical Calculations. *Int. J. Biol. Macromol.* **2020**, *157*, 1–9.

<https://doi.org/10.1016/j.ijbiomac.2020.03.251>

**Supplemental information****CARBOHYDRATE – PROTEIN AROMATIC RING INTERACTIONS BEYOND CH/ $\pi$  INTERACTIONS: A PROTEIN DATA BANK SURVEY AND QUANTUM CHEMICAL CALCULATIONS****Ivana M. Stanković, Jelena P. Blagojević Filipović, and Snežana D. Zarić**Figure S1. The example of a and b carbohydrate faces,  $\beta$ -D-glucose.

The contacts with CH/O interactions, where aromatic amino acids are hydrogen donors are prone to larger dihedral angle and offset values (Figure S2). There is no particular tendency for contacts with CH/O interactions, where carbohydrates are hydrogen donors (Figure S2). Figures S3-S5 show that smaller dihedral angle and offset values are more common for contacts with CH/N, OH/ $\pi$  and classical hydrogen bonds, respectively.

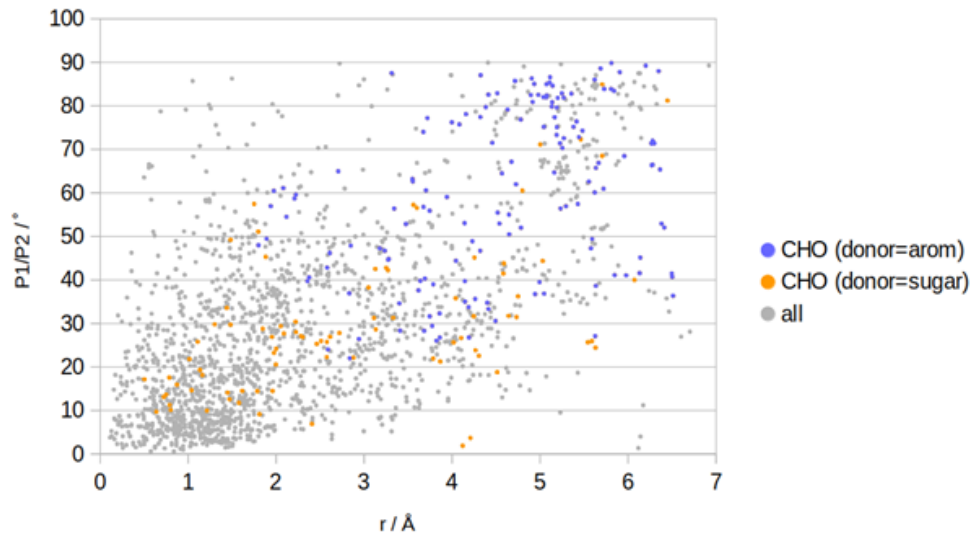


**Figure S2.** Dependences of the angles between rings on offset values, for all contacts and contacts with CH/O interactions, when hydrogen donor is the aromatic amino acid or sugar molecule

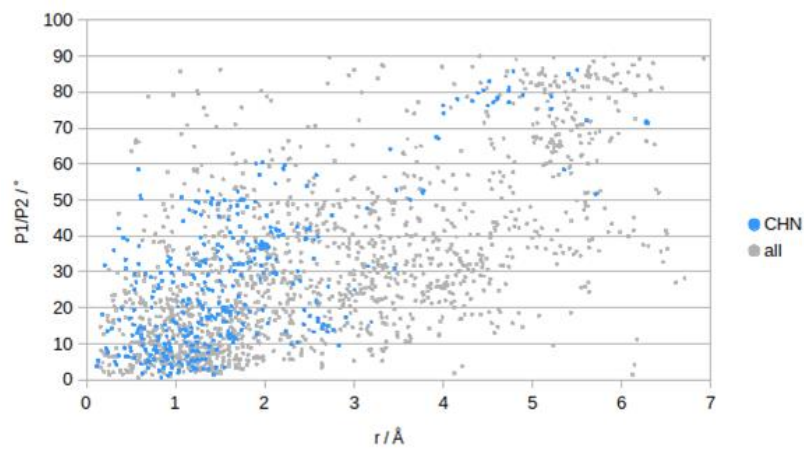


**Figure S3.** Dependences of the angles between rings on offset values, for all contacts and contacts with CH/N interactions

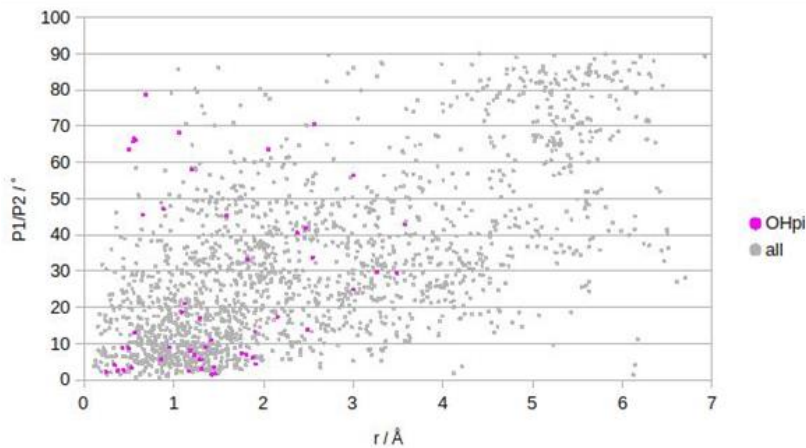


**Figure S4.** Dependences of the angles between rings on offset values, for all contacts and contacts with OH/ $\pi$  interactions

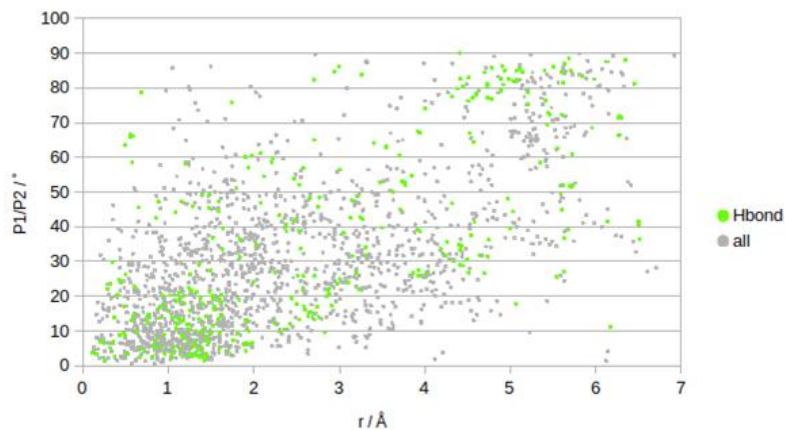


**Figure S5.** Dependences of the angles between rings on offset values, for all contacts and contacts with classical hydrogen bonds

### Higher $P_1/P_2$ angles

The sugar-aromatic contacts involving CH/ $\pi$  interactions tend to be parallel (Figure 2A, 3 and 4), as the consequence of the sugar CH group nearly perpendicular to the sugar plane. However, in some of the contacts there are higher  $P_1/P_2$  angles between rings (Figure 2A) that are the consequence of distorted high-energy sugar rings, or deoxy sugars with missing OH groups. The example is shown in Figure S6.

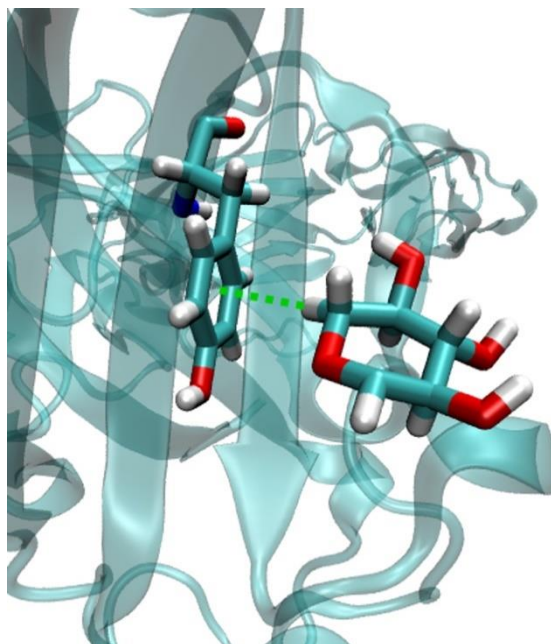


**Figure S6:** An example of the deoxy sugar forming non-parallel contact to the aromatic ring. Green dotted line represents CH/ $\pi$  interaction.

### **The distribution of the number of CH/ $\pi$ interactions**

The distribution of the number of CH/ $\pi$  interactions per sugar-aromatic pair demonstrates tendency towards only one or two CH/ $\pi$  bonds per sugar-aromatic pair (Figure S7). It means that one or two CH/ $\pi$  bonds per sugar/aromatic pair are sufficient for holding them together. PHE and TYR form only one or two, rarely three CH/ $\pi$  interactions, while TRP can form one, two, three or four because of its two aromatic rings. We plotted  $R(r)$  dependences for each one of these groups: with one, two, three or four CH/ $\pi$  interactions (Figure S7). For the higher number of CH/ $\pi$  interactions, the tendency is towards less scattered  $R$  values and lower  $r$  values, which proves that the CH/ $\pi$  interactions are responsible for tighter bonding between carbohydrate and aromatic moieties, even though one such bond is sufficient for holding the carbohydrate in place.

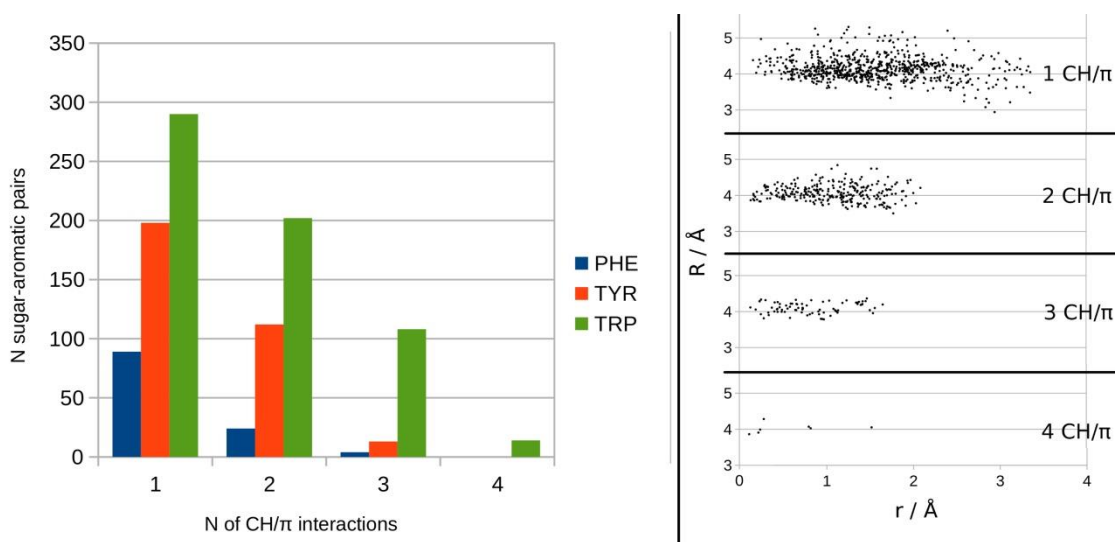


**Figure S7:** The distribution of the number of CH/π interactions per sugar-aromatic pair. The R(r) diagrams related to each number of CH/π interactions are shown on the right side.

### The sandwich aromatic amino acid/carbohydrate arrangements

The survey pointed to rare sandwich arrangements (two aromatics per sugar monomer, Figure S8) for the CH/π interacting pairs: from 1054 contacts with CH/π only 49 of them are positioned in aromatic sandwich.

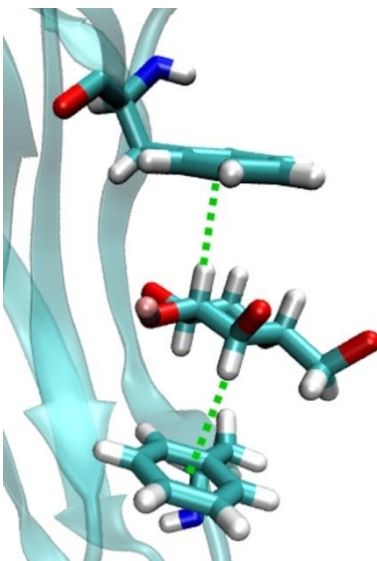


**Figure S8:** Example of sandwich interaction: two aromatic rings interacting simultaneously with one sugar ring. PDB id: 5DPN.

The graphs in Figure S9 represent the projections of monosaccharide centers onto aromatic ring plane of the six-membered rings of PHE, TYR and TRP. Data for contacts with CH/ $\pi$  interactions (Figure S9) show no specificity in offset nor  $\varphi$  angle (Figure 2B), except for TRP. The clustering in the fourth quadrant for TRP is due to interactions with five-membered TRP ring (Figure 2B, Figure S9A). The distribution of the  $\varphi$  angle in contacts without CH/ $\pi$  interactions (Figure S9B) shows that there is clustering in the second and third quadrant for all three aromatic rings, probably due to steric hindrances caused by the protein backbone.

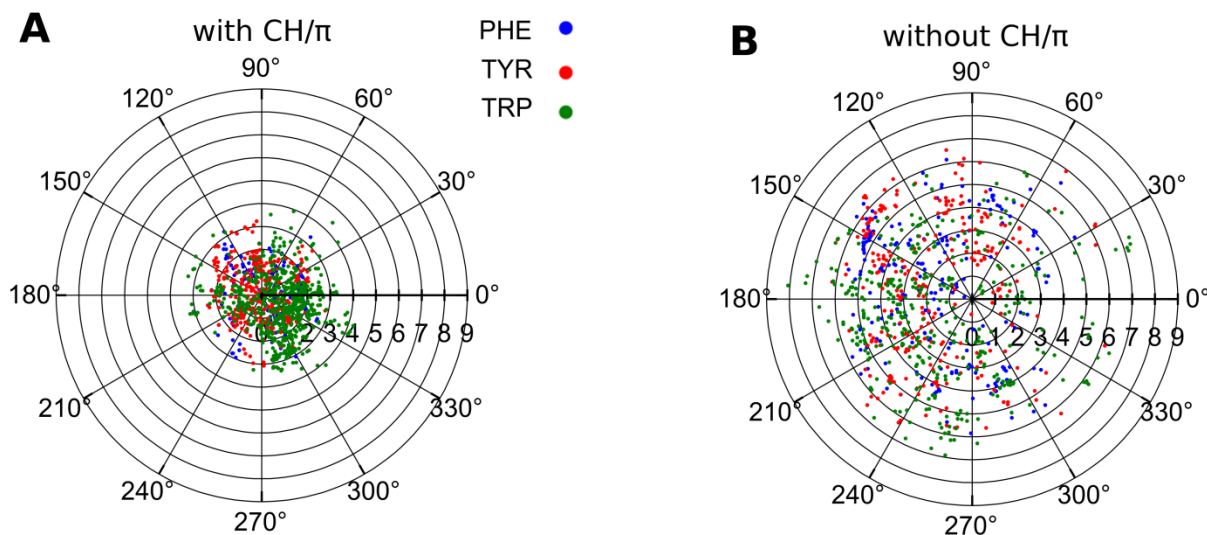


**Figure S9.** The polar graph offset -  $\varphi$  angle (Figure 2B) for the contacts involving CH/ $\pi$  interactions (A) and without CH/ $\pi$  interactions (B). Different aromatic amino acids are represented separately.

**Table S1.** Pattern of the average number of aromatic rings per carbohydrate substrate (both monomers and oligomers) and per monomer, with and without CH/ $\pi$  interactions.

Number of monomers per oligomer unit	N of substrates	Any contact		With CH/ $\pi$		Without CH/ $\pi$	
		N of aromatics per substrate	N of aromatics per monomer	N of aromatics per substrate	N of aromatics per monomer	N of aromatics per substrate	N of aromatics per monomer
1	799	0.68	0.68	0.32	0.32	0.36	0.36
2	243	1.45	0.72	0.99	0.50	0.46	0.22
3	156	1.40	0.47	0.85	0.28	0.55	0.19
4	95	1.92	0.48	1.33	0.33	0.59	0.15
5	54	2.28	0.46	1.39	0.28	0.89	0.18
6	49	3.14	0.52	1.82	0.30	1.32	0.22
7	26	2.78	0.40	1.62	0.23	1.16	0.17
8	20	2.95	0.39	1.40	0.18	1.55	0.21

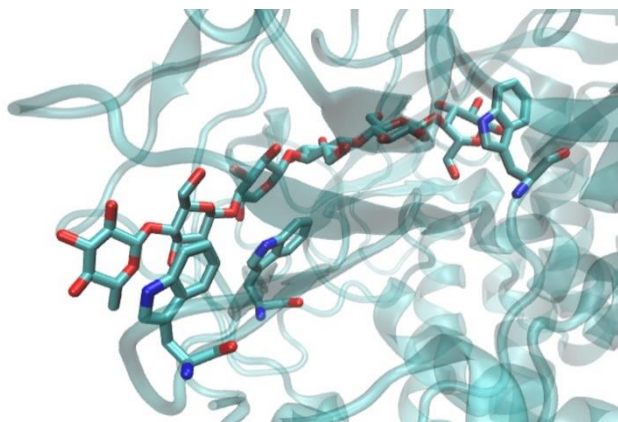


**Figure S10.** An example of a six units long carbohydrate substrate interacting with three aromatic rings in the protein cleft. PDB id: 1L2A.